Available online at www.sciencedirect.com
ScienceDirect
Tetrahedron
Tetrahedron 64 (2008) 175–185
www.elsevier.com/locate/tet

Organogelators from self-assembling peptide based dendrimers: structural and morphological features

Goutam Palui [a], François-Xavier Simon [c], Marc Schmutz [c], Philippe J. Mesini [c,*], Arindam Banerjee [a,b,*]

[a] *Department of Biological Chemistry, Indian Association for the Cultivation of Science, Jadavpur, Kolkata, West Bengal 700 032, India*
[b] *Chemistry Division, Indian Institute of Chemical Biology, Jadavpur, Kolkata, West Bengal 700 032, India*
[c] *Institut Charles Sadron, CNRS UPR22, 6, rue Boussingault, 67083 Strasbourg, Cedex, France*

Received 3 September 2007; received in revised form 27 September 2007; accepted 18 October 2007
Available online 22 October 2007

Abstract

Two peptide based dendrimers containing L-aspartic acid as the branching unit and succinic acid/terephthalic acid as the core unit were synthesized, characterized, and studied. These dendritic peptides form gels in various organic solvents including *n*-hexanol, benzene, toluene, chlorobenzene, 1,2-dichlorobenzene, *o*-xylene, tetralin, and nitrobenzene. Gels were characterized by freeze fracture transmission electron microscopic (FF-TEM), field emission scanning electron microscopic (SEM), transmission electron microscopic (TEM), wide angle X-ray powder diffraction (WAXPD), and variable temperature FTIR (VT-FTIR) studies. The VT-FTIR study indicates that amides and ester groups are involved in intermolecular hydrogen bonding in the gel state. Two transitions have been observed for both the dendrimer gels upon heating: the first one corresponds to the gel to sol transition and corresponds to the breaking of hydrogen bonds between esters and amides; the second one corresponds to the breaking of hydrogen bonds between amides. In the case of dendrimer **1** structural reorganization occurs in the sol state after the first transition, which is absent in the dendrimer **2** in the sol state. FF-TEM observations showed that both dendritic peptides form a platelet structure in gel state. SEM images of these dried gels indicate different geometry in different solvents in their self-assembled gel state.

Keywords: Dendrimer; Self-assembly; Gelation; Nanostructure

1. Introduction

Over the past 15 years, it has been recognized that the formation of gel-phase materials using self-assembling discrete 'small' molecules is one of the most exciting frontiers of supramolecular chemistry.[1] In order to generate a gel-phase material it is necessary to select or construct a molecular building block which self-assembles through various non-covalent interactions including hydrogen bonds,[2] π−π stacking,[3] metal coordination,[4] and van der Waals interactions.[5] To generate a tunable gel-phase material, it is therefore necessary to understand and modulate the specific non-covalent interactions between individual building blocks in such a way that the modulation in the molecular building blocks can be transcribed up to the nanoscale/microscale structure and ultimately to the macroscopic properties. The discovery and development of low molecular weight organogels are specially important due to numerous applications of gels as structure directing agents,[6] stabilization of organic photochromatic material,[7] in situ formation and stabilization of nanoparticle,[8] light-harvesting materials,[9] drug delivery systems,[10] dental composite carriers,[11] and in preparing dye sensitized solar cells[12] and others.[13] Dendrons and dendrimers are particularly interesting candidates for gelating the organic solvents. These dendritic gelators possess some advantages as they contain many repeating functional groups within their branched architectures.[14] Dendrons can be considered as individual dendritic branches, whilst dendrimers are structures in which a number of dendrons are attached to a single core unit and therefore their

* Corresponding authors. Tel./fax: +91 33 2473 5197 (A.B.); fax: +33 (0) 388 4140 99 (P.J.M.).
E-mail addresses: mesini@ics.u-strasbg.fr (P.J. Mesini), arindam.bolpur@yahoo.co.in, arindam@iicb.res.in (A. Banerjee).

0040-4020/$ - see front matter © 2007 Elsevier Ltd. All rights reserved.
doi:10.1016/j.tet.2007.10.061

molecular weight is considerably high. These high molecular weight dendrimers can be considered as a unique family of nanoscopic building blocks.[15] In the early 1990s, Newkome and co-workers initiated the field by reporting dendritic bola-amphiphiles with hydrophilic surfaces and hydrophobic interiors that form hydrogels.[16] In 2000, Aida and co-workers reported the first one-component dendritic gelators for organic solvent at low concentration.[17] Simanek and co-workers also reported dendritic gels based on triazines.[18] Moreover, the dendrimers based on α-amino acid units[19] are of increasing interest because of their structural resemblance to protein molecules. Such biomimetic dendrimers[20] represent a new of class material, which can act as potentially novel drug delivery agents having enhanced biocompatibilities. They have also been used as biological mimics for the exploration and understanding the biological function of proteins.[21] However, much less attention has been paid to the self-assembly of natural amino acid based dendrons and dendrimers, which form gels under suitable conditions. Smith and his co-workers have studied gel-forming polylysine dendrimers[22] and gel-forming behavior of glutamate based dendrimers has been studied by Ranganathan et al.[23] Recently, gelation property of poly (Gly–Asp) dendrons and glutamic dendrons has been studied.[24] Kim and co-workers have also used peptidic dendrons that form gel-phased assembled materials, but they form gels at relatively higher concentration (8% w/v).[25] In this paper, we present various organogels prepared from self-assembled peptide based dendritic molecules. The gel-forming behaviors of these materials have been studied using variable temperature FTIR studies in the gel-phase state, freeze fracture transmission electron microscopic (FF-TEM), field emission scanning electron microscopic (FE-SEM), high resolution transmission electron microscopic (HR-TEM), and wide angle X-ray powder diffraction (WAXPD) studies.

2. Results and discussion

2.1. Synthesis

The dendrimers based on L-aspartic acid were synthesized in optically pure form according to Scheme 1 using a convergent coupling methodology. Solution-phase approach was

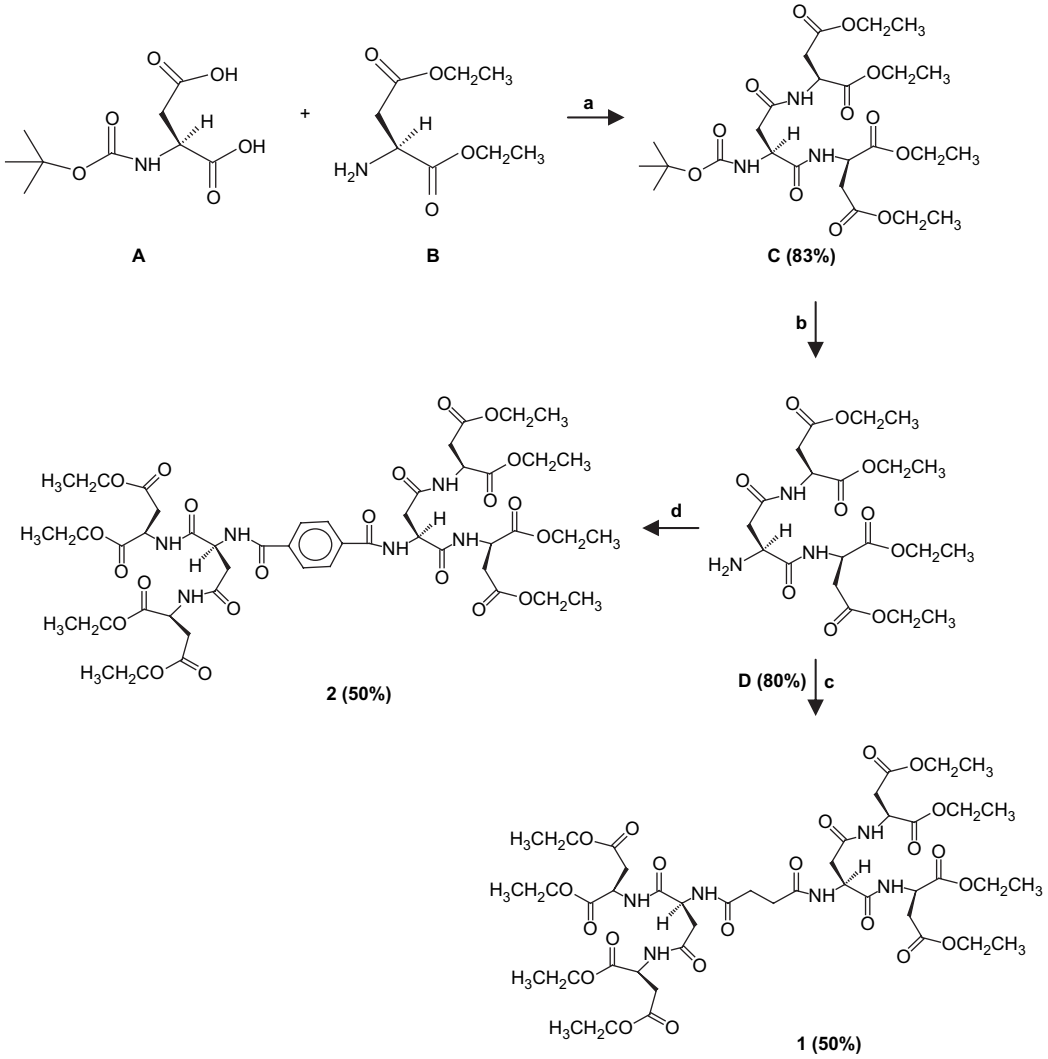

Scheme 1. Convergent synthesis of dendrimers **1** and **2**. Reagents and conditions: (a) HOBt, DCC; (b) TFA, $NaHCO_3$; (c) succinic acid, HOBt, DCC; (d) terephthalic acid, HOBt (*N*-hydroxybenzotriazole), DCC (*N*,*N*-dicyclohexylcarbodiimide).

used to get the desired compounds.[26] DCC (1,3-dicyclohexylcarbodiimide) was used as coupling agent and HOBt (1-hydroxybenzotriazole) was used to suppress the racemization of the chiral centers. The final products were purified by column chromatography using silica (100–200-mesh size) gel as stationary phase and chloroform–methanol (95:5) mixture as eluent and the products were characterized using ^{1}H NMR, ^{13}C NMR, and HRMS techniques.

2.2. Thermal behavior of the gel-phase materials

The dendrimeric molecules **1** and **2** are readily soluble in different organic solvents with increasing the temperature and when the solutions were allowed to cool at room temperature, gels are obtained within half an hour. The gelling propensity of these reported dendrimers (**1** and **2**) in a wide range of organic solvents including *n*-hexanol, toluene, *ortho*-dichlorobenzene (*o*-DCB), chlorobenzene, nitrobenzene, tetralin, and *o*-xylene was studied by dissolving a small amount (<2% w/v) of compounds in the desired solvent under heating. Upon cooling to below room temperature (30 °C), the complete volume of the respective solvent is immobilized and formed a gel. The gelation was confirmed by the inverted test-tube method. Dendrimer **1** forms gels in those solvents at fairly low concentrations (<1% w/v) (Table 1). The 'tube inversion' method was used to measure sol–gel transition temperature (T_{gel}) of all the gel-phase materials (**1** and **2**) in different organic solvents at different concentrations. The measured temperatures are plotted against the gelator concentration to afford the phase diagrams presented in Figure 1 in a specific representation $\ln(\phi_{ag})$ versus T (ϕ_{ag} being the unit mole fraction of gelator and T is the corresponding gel melting temperature). This specific representation is convenient when thermodynamic parameters of the aggregates will be determined, since they are proportional to the slope $\delta \ln(\phi_{ag})/\delta T$ [see Eq. 1].

$$\Delta G^{0}_{ag} = RT \ln(\phi_{ag}) \quad (1a)$$

$$\Delta H^{0}_{ag} = -RT^{2}\left(\delta \ln(\phi_{ag})/\delta T\right) \quad (1b)$$

$$\Delta S^{0}_{ag} = -R \ln(\phi_{ag}) - RT\left(\delta \ln(\phi_{ag})/\delta T\right) \quad (1c)$$

Table 1
Gelation properties of dendrimers **1** and **2** in organic solvents[a]

Solvent	**1**	**2**
Methanol	S	S
Ethanol	S	S
n-Hexanol	G(0.83)	G(0.55)
o-DCB	G(0.45)	G(0.83)
Chlorobenzene	G(0.56)	G(0.83)
Nitrobenzene	G(0.50)	G(1.67)
Toluene	G(0.83)	G(1.67)
o-Xylene	G(0.71)	G(0.55)
Tetralin	G(0.63)	G(0.56)
Benzene	G(0.55)	I

[a] G: stable gel formed at room temperature, in parentheses: minimum gelation concentration (% w/v), S: soluble, I: insoluble.

T is the absolute temperature, ΔG^{0}_{ag} is the standard free energy, ΔH^{0}_{ag} is the standard free enthalpy, and ΔS^{0}_{ag} is the entropy of formation of the aggregates through a phase separation process. Tables 2 and 3 show the enthalpy and entropy values of **1** and **2** in different solvents. Interestingly, these calculated values show that there is clear enthalpy–entropy compensation. When the enthalpy is large and favorable, the entropy is large and unfavorable and when enthalpy is small, so is the entropy. This is often seen in binding processes. A comparison of the phase diagrams of a particular gelator shows that standard free energies differ in different organic solvents, which suggests that mechanism of aggregation is different in different solvents.[27] The enthalpy values found by this method are of the order of the magnitude of reversible bonds such as hydrogen bonds between amides (ca. 15 kJ mol^{-1}).

2.3. VT-IR studies

The IR spectra of the gels of the dendrimers **1** and **2** in 1,2-dichlorobenzene gels (1% w/v) were recorded at different temperatures. The IR spectrum of the gel (dendrimer **1**) at low temperature (Fig. 2) in the NH stretching area shows only one major band at 3283 cm^{-1} that is characteristic of a hydrogen-bonded amide. The carbonyl stretching area shows a major peak at 1641 cm^{-1}, corresponding to a shift of the amide I band of hydrogen-bonded amide. The spectrum at low temperatures also shows two shifts for the bands of the ester carbonyls 1731.3 cm^{-1} and 1737.2 cm^{-1}. This demonstrates that there are two sets of ester groups. The lower frequency shift can be attributed to hydrogen-bonded ester groups and the higher to free ester groups. The corresponding NH band should be found at higher frequencies (in usual solvents up to 3390 cm^{-1}). It is not visible on the figure, but might lie under the tail of the major peak around 3350 cm^{-1}.

When the temperature is increased (Fig. 2), the NH stretching band has a maximum that shifts slightly and gradually up to 3286.8 cm^{-1}, and from 92 °C to 101 °C a steeper increases to 3293.7 cm^{-1}. The carbonyl band also shows a steep increase although more modest in magnitude (from 1641.5 cm^{-1} to 1643.6 cm^{-1}). The most important spectral change in the carbonyl stretching area in this temperature range concerns the relative intensities of the two bands of the esters. The ratio of the intensities of the two different ester bands shows a steeper increase from 92 °C to 101 °C (Fig. 3, bottom). These changes allow the clear identification of a transition at a temperature of 95 °C, which is also observed from the phase diagram (gel to sol transition). The intensities of the amide A and amide I bands do not show a significant decrease after the transition (Fig. 3). On the contrary the intensity increases from 95 °C to 104 °C (Figs. 2 and 3, top). The increase of the amide I band at 1643 cm^{-1} is highlighted in the difference spectra (Fig. 4). The same behavior is observed for the maximum of the amide I band at 1643 cm^{-1} on Figure 2 and is highlighted by the differential representation (Fig. 4). These spectral modifications show that after the transition the amide groups remain linked by hydrogen bonds.

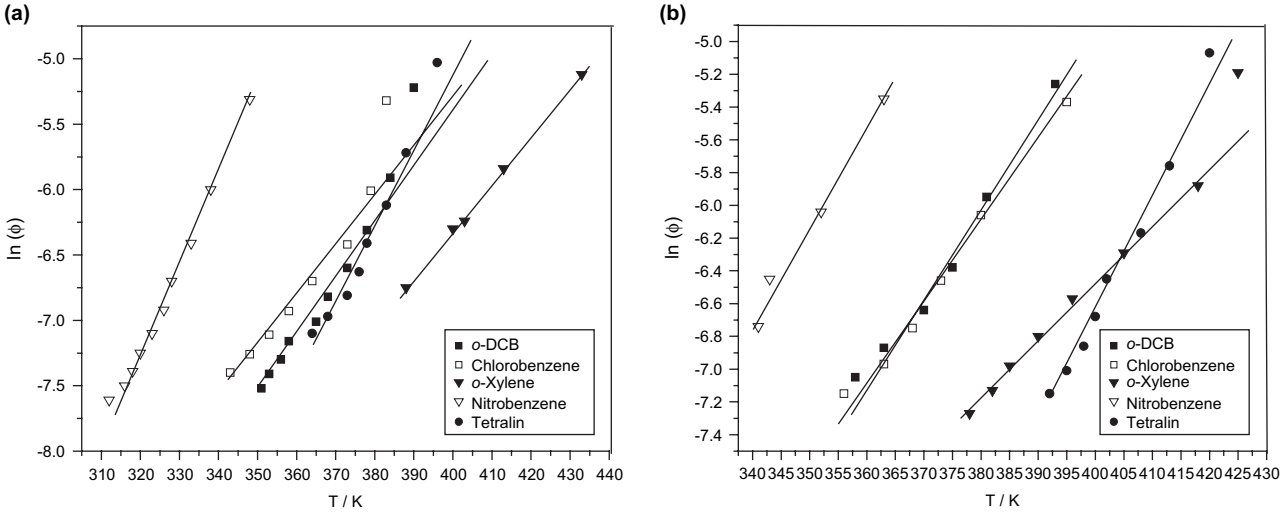

Figure 1. (a) Concentration–temperature phase diagrams $\ln(\phi_{ag})$ versus T of dendritic gelator **1** in different solvents and (b) concentration–temperature phase diagrams $\ln(\phi_{ag})$ versus T of dendritic gelator **2** in different solvents.

Table 2
Gel/sol phase diagrams [$\ln(\phi_{ag})$[a] vs T] of dendrimer **1**

Solvent	$\delta \ln(\phi_{ag})/\delta T$[b]	ΔH^0_m[c]/kJ mol^{-1}	$\ln(\phi_{ag})$[a]	ΔS^0_m[d]/JK^{-1} mol^{-1}	ΔG^0_m[e]/kJ mol^{-1}
o-Dichlorobenzene	0.047198	−53.1	−6.82	−87.7	21.0
Chlorobenzene	0.035828	−38.2	−6.93	−49.0	20.6
o-Xylene	0.033984	−42.5	−6.75	−53.5	21.8
Nitrobenzene	0.069129	−61.1	−6.92	−129.8	18.8
Tetralin	0.069411	−82.5	−6.63	−161.9	20.8

[a] ϕ_{ag} is the unit mole fraction; T is in K.
[b] $\delta \ln(\phi_{ag})/\delta T$ is the slope of the phase diagram (K^{-1}).
[c] ΔH^0_m is the standard enthalpy for the melting transition of the gels.
[d] ΔS^0_m is the standard entropy for the melting transition of the gels.
[e] ΔG^0_m is the standard free energy for the melting transition of the gels.

However, the displacements of the shifts of the NH stretching and the amide I bands show that the hydrogen bonds strongly reorganize. The outlook of all the measured spectra shows a second transition that occurs around 120 °C. The ratio of the intensities of the bands at 1742 cm^{-1} and 1728 cm^{-1} also shows a steep increase. When the temperature reaches 122 °C, the NH band transforms into two bands at 3354 cm^{-1} and 3418 cm^{-1}. The higher frequency band can be attributed to free NH. The meaning of the lower band is less obvious. Similar bands can be observed in nylons during the Brill transition. They are related to amides linked through hydrogen bonds that are weakened because of the disorder induced by the chains by temperature.[28] In the carbonyl region the peak with the maximal intensity is found at 1680 cm^{-1}, but a large contribution at 1660 cm^{-1} is also observed, which shows that the amides are organized in two different ways.

The IR spectra of the dendrimer **2** also show that, in the gel state, most of the amides are bonded through hydrogen bonds (Fig. 5, top) and that part of the ester groups is hydrogen-bonded (Fig. 5, bottom), while the other part is free. The

Table 3
Gel/sol phase diagrams [$\ln(\phi_{ag})$[a] vs T] of dendrimer **2**

Solvent	$\delta \ln(\phi_{ag})/\delta T$[b]	ΔH^0_m[c]/kJ mol^{-1}	$\ln(\phi_{ag})$[a]	ΔS^0_m[d]/JK^{-1} mol^{-1}	ΔG^0_m[e]/kJ mol^{-1}
o-Dichlorobenzene	0.043950	−48.2	−6.87	−75.5	20.7
Chlorobenzene	0.052047	−57.0	−6.97	−99.1	21.0
o-Xylene	0.034490	−43.6	−6.80	−55.3	22.1
Nitrobenzene	0.062531	−60.5	−6.74	−121.2	19.1
Tetralin	0.070373	−93.6	−6.68	−178.5	22.2

[a] ϕ_{ag} is the unit mole fraction; T is in K.
[b] $\delta \ln(\phi_{ag})/\delta T$ is the slope of the phase diagram (K^{-1}).
[c] ΔH^0_m is the standard enthalpy for the melting transition of the gels.
[d] ΔS^0_m is the standard entropy for the melting transition of the gels.
[e] ΔG^0_m is the standard free energy for the melting transition of the gels.

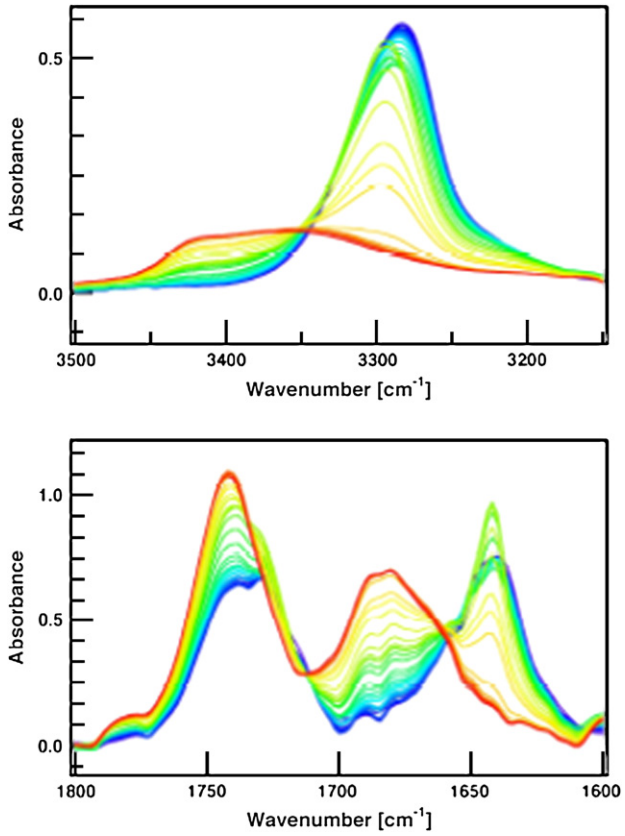

Figure 2. IR spectra of 1% gel of dendrimer **1** in DCB at temperatures from 32 °C (———) to 140 °C (———). Top: NH stretching area. Bottom: CO stretching area.

evolution of the spectra when the temperature increases indicates two transitions. The first one occurs at about 90 °C, which is similar to the value of 89 °C observed from the phase diagram (Fig. 1). The second one occurs at 130 °C. The first

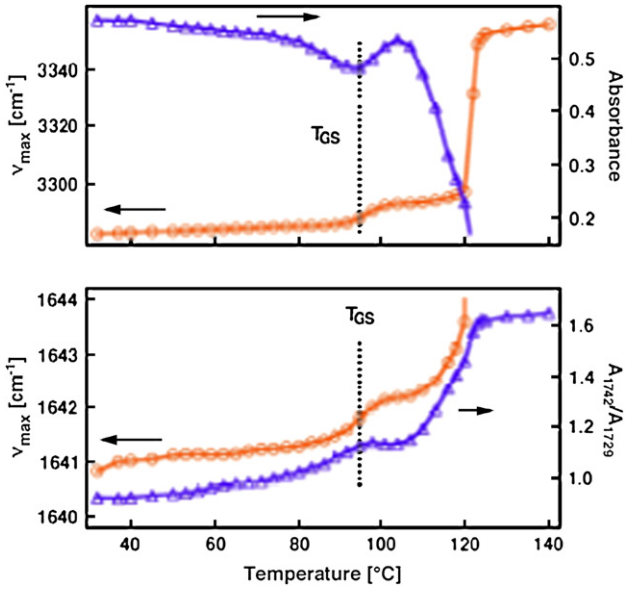

Figure 3. Gel of **1** in DCB (1% w/v): variation of spectral features with *T*. Top: ○: shift of the max. NH band, △: absorbance of the maximum. Bottom: ○: shift of the max. Amide I band, △: ratio of the absorbance of the bounded ester bond (1742 cm^{-1}) to free ester bonds (1729 cm^{-1}).

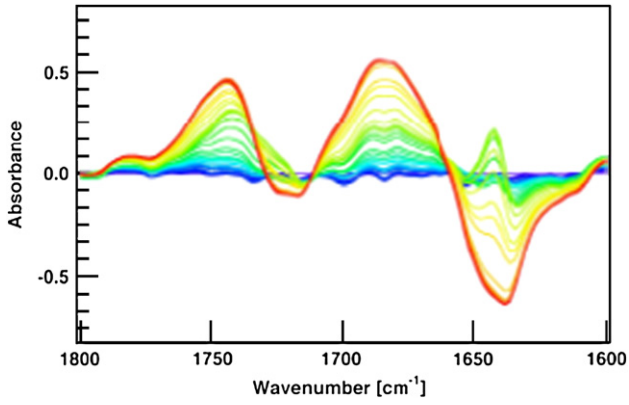

Figure 4. Differential IR spectra of 1% gel of dendrimer **1** in DCB at temperatures from 32 °C (———) to 140 °C (———).

transition is coincident with the transformation of hydrogen-bonded esters to free ones. This can be seen in Figure 6 (bottom). However, here the shift of the amide I shows almost no change (from 1639.2 cm^{-1} to 1639.6 cm^{-1}) from 60 °C to 110 °C (Fig. 6, bottom) and its intensity decreases. During the gel to sol transition, unlike for the dendrimer **1**, the amides that are no longer hydrogen-bonded to the ester groups do not reorganize and their intensity tends to decrease slightly. The second transition is comparable with what happens with dendrimer **1**. However, the ratio of the intensity at 3354 cm^{-1} to

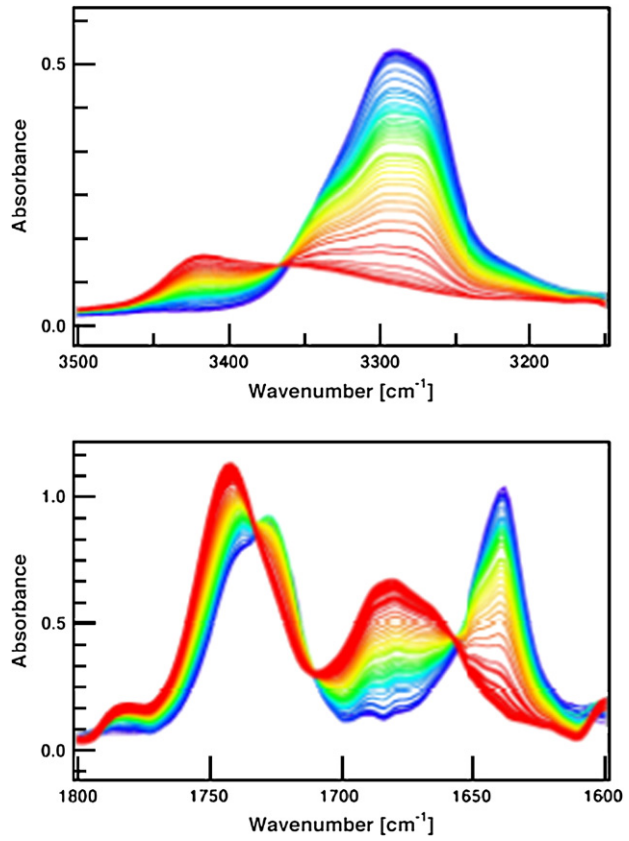

Figure 5. IR spectra of 1% gel of dendrimer **2** in DCB at temperatures from 40 °C (———) to 140 °C (———). Top: NH stretching area. Bottom: CO stretching area.

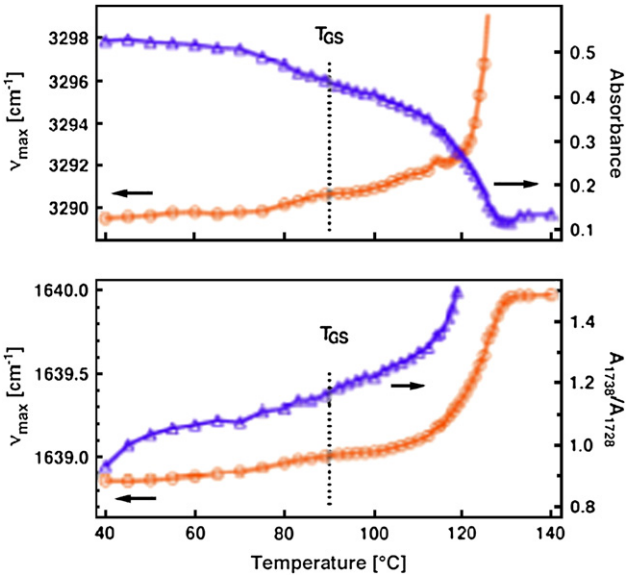

Figure 6. Gel of **1** in DCB (1% w/v): variation of spectral features with *T*. Top: ○: shift of the max. NH band, △: absorbance of the maximum. Bottom: ○: shift of the max. Amide I band, △: ratio of the absorbance of the bounded ester bond (1738 cm^{-1}) to free ester bonds (1728 cm^{-1}).

the intensity at 3418 cm^{-1} is higher for dendrimer **2**, thus showing that the dendrimer **2** forms more free amides.

To conclude this VT-IR study, for both dendrimers the intermolecular interactions that are responsible for the gel state are hydrogen bonds between esters and amides and between amides and amides. The gel to sol transition corresponds to the breaking of a few hydrogen bonds between amides and esters. This leads to a reorganization of the hydrogen bonds between the amides. The resulting bonds are likely intramolecular, since they happen in the sol state. For dendrimer **2**, the breaking of the amide-to-ester hydrogen bonds does not lead to any reorganization. The core of the dendrimer can perhaps explain the difference in behavior between both dendrimers. For dendrimer **2** the rigidity of the central aromatic ring impedes the ability to fold and make new intramolecular hydrogen bonds between the amides. The energy of a hydrogen bond[29] between an ester and an amide is about 12 kJ mol^{-1}. This is weaker than the hydrogen bonds formed between amides and explains why these bonds break first.

2.4. Wide angle X-ray diffraction study

Figure 7 demonstrates the X-ray diffraction pattern obtained from dendrimers **1** and **2** in three different states (bulk solid powder, gel in *ortho*-dichlorobenzene, and xerogel in the same solvent) and the major peaks are listed in Table 4. It was found that the structure in the bulk solid and the dried gel is somewhat similar. The powder of dendrimer **2** shows a better ordering than the dendrimer **1**. As no distances have been detected between 3.4 Å and 3.8 Å from this diffractogram, we can conclude that there is no clear π–π interaction between the aromatic units in the self-assembled form of dendrimer **2**.

In the solid state of dendrimer **1**, it is visible that the minimum distance for dendrimer is only 11.4 Å, which is much shorter than the length of the molecule in a extended conformation where the maximal length is 24 Å. This is coherent with a molecule that can be backfolded. The structure in the wet gel state is different from those in the dried gel and solid state structures. These figures confirm that the molecular arrangements of the fibers in gel state are distinctly different from that of the fibers obtained from the bulk solid or dried gel.[17b,30]

2.5. Morphology and characterization

To obtain visual images of the assembled dendrimers **1** and **2** from various organic solvents, the morphologies of the xerogels obtained from both dendritic compounds were

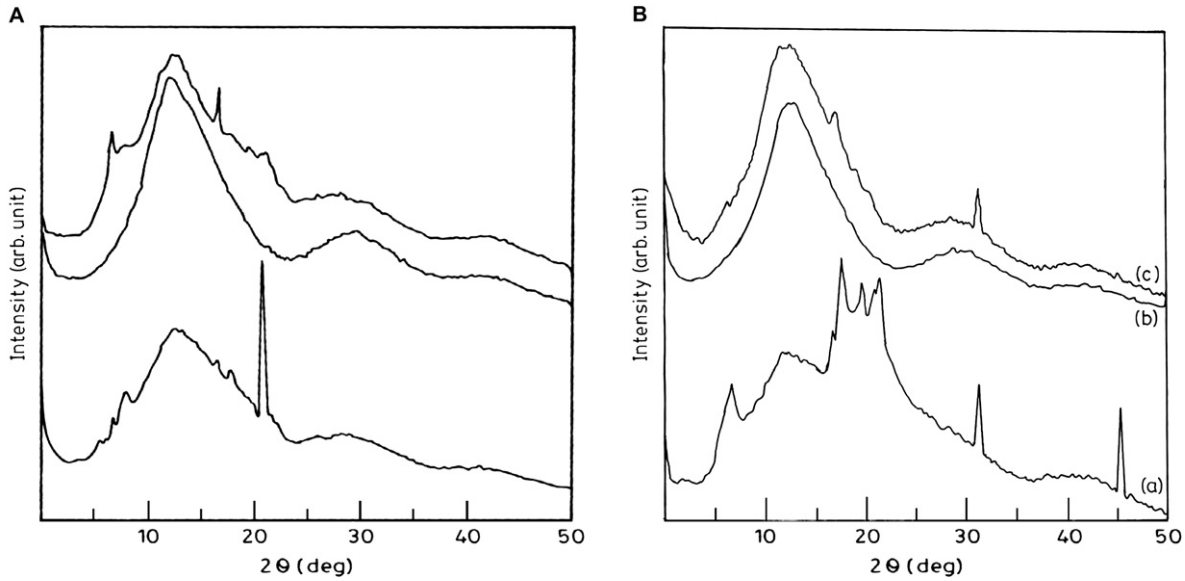

Figure 7. X-ray powder diffraction pattern of (A) dendrimer **1** and (B) dendrimer **2** in their (a) bulk solid, (b) wet gel, and (c) dried gel conditions.

Table 4
Major peaks in the XRD pattern for dendrimers **1** and **2** in various conditions

Dendrimer	*d*-Spacing [Å]
1	Bulk solid: 11.39, 9.96, 6.71, 5.14, 4.78, 4.14, 4.02, 3.02, 2.18 Wet gel: 6.79, 2.97 Dried gel: 11.43, 6.75, 5.12, 4.06, 3.09
2	Bulk solid: 29.43, 11.54, 6.70, 5.11, 4.87, 4.38, 4.05, 2.82, 2.35, 1.99 Wet gel: 6.48, 3.07, 2.18 Dried gel: 11.47, 6.40, 3.01, 2.82, 2.26, 1.99

investigated by field emission scanning electron microscopic (FE-SEM) studies. The FE-SEM images of xerogel obtained from dendrimers **1** and **2** in different solvents (Fig. 8) show their nanoscale assembly. Dendrimers **1** and **2** form fibrous nanoscale architecture. The micrographs of the dried gels are strongly dependent on the gelling solvents. Xerogels of **1** and **2** from nitrobenzene show tape-like morphology of about 350–470 nm and 270–320 nm in width, respectively. On the other hand, the xerogel obtained from *ortho*-xylene shows

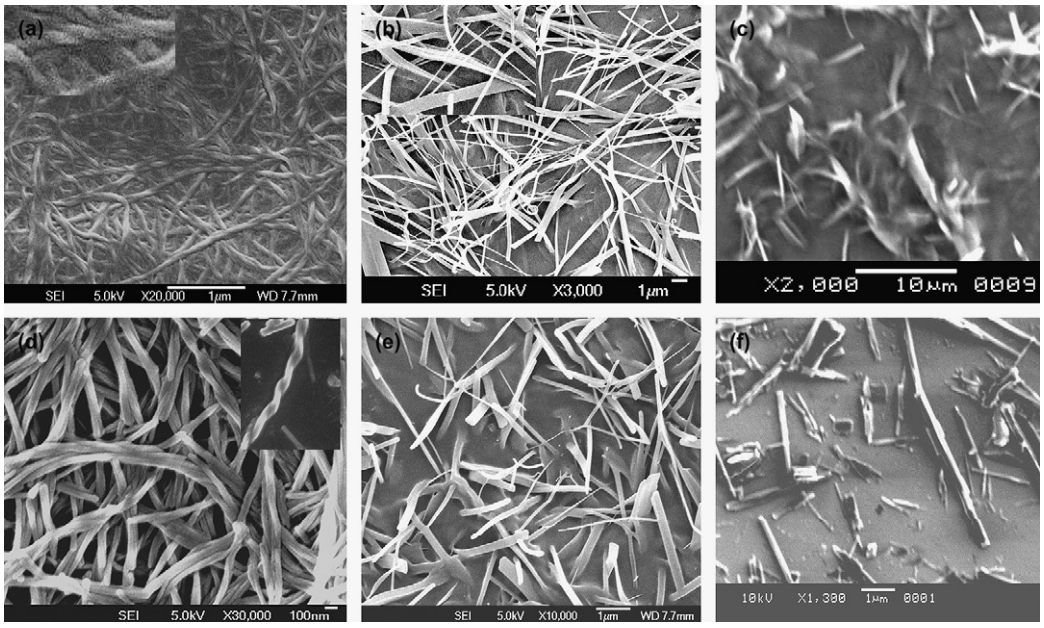

Figure 8. Field emission scanning electron microscopic (FE-SEM) images of xerogels derived from (a) dendrimer **1** in *o*-xylene (1% w/v), (b) dendrimer **1** in *o*-dichlorobenzene (1% w/v), (c) dendrimer **1** in nitrobenzene (1% w/v), (d) dendrimer **2** in *o*-xylene (1% w/v), (e) dendrimer **2** in *o*-dichlorobenzene (1% w/v), and (f) dendrimer **2** in nitrobenzene (1% w/v).

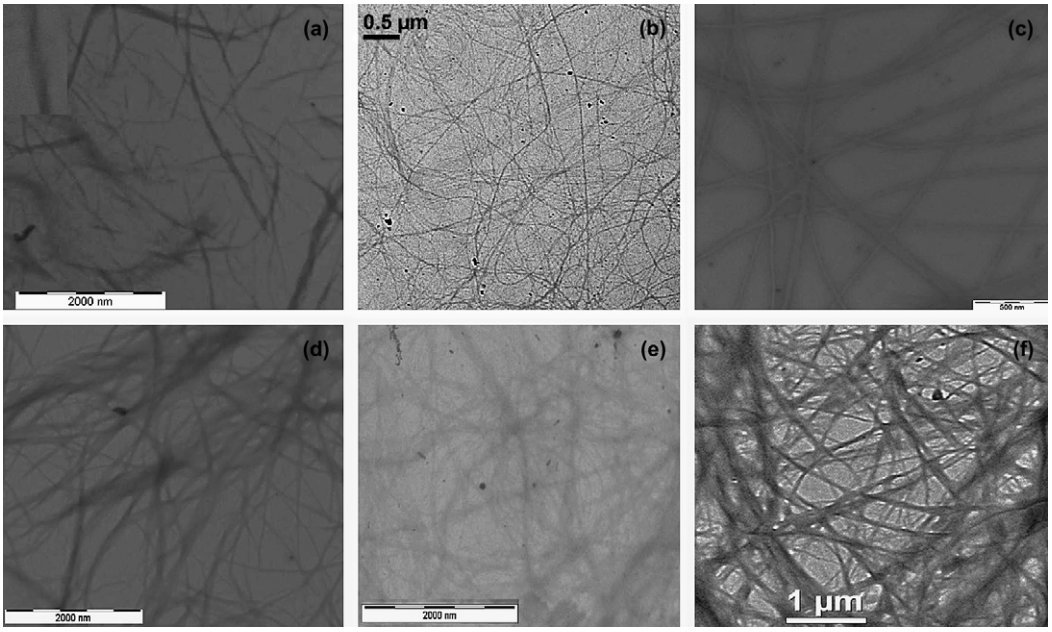

Figure 9. Transmission electron microscopic (TEM) images of xerogels derived from (a) dendrimer **1** in *o*-xylene, (b) dendrimer **1** in nitrobenzene, (c) dendrimer **1** in *o*-dichlorobenzene, (d) dendrimer **2** in *o*-xylene, (e) dendrimer **2** in nitrobenzene, and (f) dendrimer **2** in *o*-dichlorobenzene.

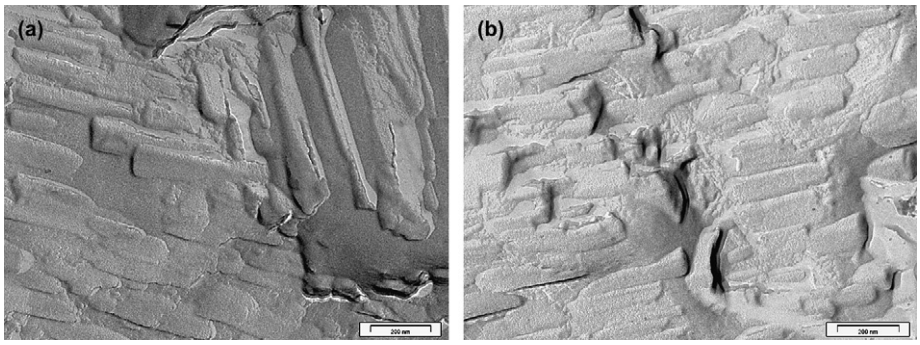

Figure 10. Internal structure of the gels revealed and visualized by FF-TEM. Gels derived from (a) dendrimer **1** in *ortho*-dichlorobenzene (1% w/v) and (b) dendrimer **2** in *ortho*-dichlorobenzene (1% w/v).

a nanofibrillar network with a twisted geometry. It should be noted that each fiber consists of a bundle of much thinner fibrils with a range of diameters of 45–75 nm and 50–80 nm in the case of dendrimers **1** and **2**, respectively. Moreover these fibrils are found to be several hundreds of nanometers long, indicating the effective unidirectional 'stacking' of gelator units in the assembled state. The helical twist that has been observed is very interesting, since it is very common to biological organisms.[31] This method further throws lights on the different morphologies that can be obtained from gel-phase materials in different solvents. When we go to the different solvent systems, the morphology also changes due to different mode of aggregation in different solvents.

TEM images of xerogels of dendrimers **1** and **2** in different solvents also show nanofibrillar networks (Fig. 9) in their gel state. Interestingly, when using freeze fracture TEM, the gel state at room temperature can be observed as a three dimensional network of platelets. The gel-phase network formed in 1,2-dichlorobenzene solvent is illustrated in Figure 10a and b. The structures formed by **1** are found to be approximately 100 nm large and 20 nm thick and the length up to 1 μm long. Large areas of amorphous solvent are seen between the structures (Fig. 10a). The objects formed by **2** are around 80 nm large and vary in thickness from 10 nm to 60 nm. Their length is at least up to 0.5 μm (Fig. 10b). On the basis of these results, we can see that the morphology of the gel-phase materials strongly not only depends on the nature of the gelling solvents[32] but also on the sample preparation.[33]

3. Conclusions

A one-component dendritic gelator unit self-organizes to form supramolecular assemblies in aprotic organic solvents (i.e., benzene, chlorobenzene, *ortho*-dichlorobenzene, *ortho*-xylene, etc.). Gel material at low w/v percentage can be obtained by these dendrimeric moieties based on peptides. From FE-SEM and FF-TEM experiments, the nano-features of the gel-phase material have been observed. FE-SEM also illustrates the helical nature of the gel-forming fibers. FTIR showed that in the gel state, hydrogen bonding exists between amides and also between amide and ester. For the both dendrimers, the gel to sol transition was shown by FTIR to correspond to the breaking of the hydrogen bonds between esters and amides. For dendrimer **1**, during the transition, the hydrogen bonds between ester and amides transform into H-bonds between amides, and all the amides reorganize. For dendrimer **2** the same bonds remain. For both dendrimers after the transition, many hydrogen bonds between amide groups are preserved in the sol, which suggests that these bonds are intramolecular. A second transition at higher temperature is observed. This is associated to the breaking of part of the hydrogen bonds between amides. Further research will attempt to control the self-assembly behavior of a peptidic dendrimer based gelator unit by modifying the functional groups which are responsible for gelation and to address the question of how the molecular structure regulates the gel stability and gel formation behavior.

4. Experimental section

4.1. General methods and materials

Succinic acid, terephthalic acid, HOBt (1-hydroxybenzotriazole), DCC (dicyclohexyl carbodiimide), amino acids, and Boc-aspartic acid were purchased from Sigma chemicals.

4.2. Synthesis

The dendritic L-aspartic acid derivatives with ethyl protecting groups on the surface were synthesized (Scheme 1) by conventional solution-phase method by using racemization-free fragment condensation strategy. The Boc group was used for N-terminal protection and the C-terminus was protected as ethyl ester.[26] Couplings were mediated by dicyclohexylcarbodiimide–1-hydroxybenzotriazole (DCC/HOBt). All intermediates were characterized by ^{1}H NMR (300 MHz) and thin layer chromatography (TLC) on silica gel and used without further purification. The final products (dendrons) were purified by column chromatography using silica (100–200-mesh size) gel as stationary phase and chloroform–methanol (95:5) mixture as eluent. The purified dendrons have been fully characterized by 300 MHz ^{1}H and ^{13}C NMR spectroscopy.

4.3. Synthesis of dendrons

4.3.1. Compound *C*

A sample of Boc-Asp-OH (2.33 g, 10 mmol) dissolved in dimethylformamide (DMF) (30 mL) was cooled in an ice-water bath and H-Asp-OEt (**B**) was isolated from 1.84 g (13.2 mmol) of the corresponding ethyl ester hydrochloride by neutralization and subsequent extraction with ethyl acetate and the ethyl acetate extract was concentrated to 8 mL. It was then added to the reaction mixture, followed immediately by DCC (4.12 g, 20.0 mmol) and HOBt (2.70 g, 20.0 mmol). The reaction mixture was stirred for 3 days. The residue was taken up in ethyl acetate (40 mL) and the DCU was filtered off. The organic layer was washed with 2 M HCl (3×40 mL), brine (2×50 mL), 1 M sodium carbonate (3×40 mL), brine (2×40 mL), dried over anhydrous sodium sulfate, and evaporated in vacuum to yield **C** as a white solid. Purification was done by silica gel column (100–200 mesh) using chloroform–methanol (95:5) as eluent.

Yield=4.77 g (8.3 mmol, 83%). ^{1}H NMR ($CDCl_3$, 300 MHz, δ ppm): 1.23–1.31 (m, 12H), 1.45 (s, 9H), 2.75–3.03 (m, 6H), 4.12–4.25 (m, 8H), 4.78–4.83 (m, 3H), 6.01 (d, J=6.9, 1H), 6.74 (d, J=8.1, 1H), 7.58 (d, J=7.8, 1H). Anal. Calcd for $C_{25}H_{41}N_3O_{12}$ (575.3): C, 52.15; N, 7.30; H, 7.13. Found: C, 52.18; N, 7.29; H, 7.21. MS (HRMS) *m/z* 576.0724 $(M+H)^+$, *m/z* 599.0183 $(M+Na)^+$.

4.3.2. Compound *D*

Trifluoroacetic acid (5 mL) was added to **C** (2.88 g, 5.00 mmol) and the removal of Boc group monitored by TLC. After 2 h, trifluoroacetic acid was removed under vacuum. The residue was taken in water (20–30 mL) and washed with diethyl ether (2×30 mL). The pH of the aqueous solution was then adjusted to 8 with sodiumbicarbonate solution. The aqueous solution was extracted with ethyl acetate (3×30 mL), dried over anhydrous sodium sulfate, and evaporated in vacuum to yield the white solid **D**.

Yield=1.90 g (4.0 mmol, 80%). ^{1}H NMR (DMSO-d_6, 300 MHz, δ ppm): 1.13–1.19 (m, 12H), 2.65–2.76 (m, 6H), 4.02–4.10 (m, 8H), 4.22–4.24 (m, 2H), 4.58–4.65 (m, 1H), 7.83 (br, 1H), 8.08 (br, 1H), 8.47–8.49 (d, J=7.9, 1H). Anal. Calcd for $C_{20}H_{33}N_3O_{10}$ (475.3): C, 50.49; N, 8.84; H, 6.94. Found: C, 50.32; N, 9.12; H, 6.54. MS (HRMS) *m/z* 476.2671 $(M+H)^+$, *m/z* 498.2023 $(M+Na)^+$.

4.4. Synthesis of dendrimers

4.4.1. Synthesis of *1*

A sample of succinic acid (0.236 g, 2 mmol) dissolved in dimethylformamide (DMF) (15 mL) was cooled in an ice-water bath and **D** (2.90 g, 4.0 mmol) was then added to the reaction mixture, followed immediately by DCC (0.82 g, 4.0 mmol) and HOBt (0.54 g, 4.0 mmol). The reaction mixture was stirred for 3 days. The residue was taken up in ethyl acetate (40 mL) and the DCU was filtered off. The organic layer was washed with 2 M HCl (3×40 mL), brine (2×50 mL), 1 M sodium carbonate (3×40 mL), brine (2×40 mL), dried over anhydrous sodium sulfate, and evaporated in vacuum to yield **1** of white solid. Purification was done by silica gel column (100–200 mesh) using chloroform–methanol (95:5) as eluent.

Yield=2.07 g (2 mmol, 50.0%). $[\alpha]_D^{20}$ −22.5 (*c* 0.5, MeOH). ^{1}H NMR ($CDCl_3$, 300 MHz, δ ppm): 1.22–1.28 (m, 24H), 2.55 (s, 4H), 2.80–2.98 (m, 12H), 4.10–4.24 (m, 16H), 4.78–4.86 (m, 6H), 7.16 (d, J=8.2, 2H), 7.45 (d, J=7.8, 2H), 7.77 (d, J=8.3, 2H). ^{13}C NMR (75 MHz, rt, $CDCl_3$, δ ppm): 14.05, 14.07, 14.08, 14.11, 31.61, 33.96, 36.25, 37.29, 48.82, 49.04, 50.25, 61.04, 61.10, 61.78, 61.87, 170.53, 170.53, 170.65, 170.71, 170.82, 170.94, 172.30. Anal. Calcd for $C_{44}H_{68}N_6O_{22}$ (1033.02): C, 53.28; N, 7.77; H, 6.29. Found: C, 53.25; N, 7.78; H, 6.30. MS (HRMS) *m/z* 1033.0043 $(M)^+$, *m/z* 1055.9596 $(M+Na)^+$.

4.4.2. Synthesis of *2*

A sample of terephthalic acid (0.33 g, 2 mmol) dissolved in dimethylformamide (DMF) (15 mL) was cooled in an ice-water bath and **D** (1.90 g, 4.0 mmol) was then added to the reaction mixture, followed immediately by DCC (0.82 g, 4.0 mmol) and HOBt (0.54 g, 4.0 mmol). The reaction mixture was stirred for 3 days. The residue was taken up in ethyl acetate (40 mL) and the DCU was filtered off. The organic layer was washed with 2 M HCl (3×40 mL), brine (2×50 mL), 1 M sodium carbonate (3×40 mL), brine (2×40 mL), dried over anhydrous sodium sulfate and evaporated in vacuum to yield **2** of white solid. Purification was done by silica gel column (100–200 mesh) using chloroform–methanol (95:5) as eluent.

Yield=2.16 g (2 mmol, 50.0%). $[\alpha]_D^{20}$ −10.7 (*c* 0.5, MeOH). ^{1}H NMR ($CDCl_3$, 300 MHz, δ ppm): 1.21–1.29 (m, 24H), 2.77–3.01 (m, 12H), 4.07–4.24 (m, 16H), 4.81–4.86 (m, 6H), 5.02 (m, 2H), 7.00 (d, J=8.2, 2H), 7.84 (d, J=5.9, 2H), 7.88 (s, 4H), 8.23 (d, J=7.3, 2H). ^{13}C NMR (75 MHz, rt, $CDCl_3$, δ ppm): 14.00, 14.05, 14.07, 14.12, 33.90, 36.20, 37.21, 48.86, 48.98, 50.46, 61.02, 61.12, 61.84, 61.92, 127.50, 127.58, 166.32, 170.40, 170.42, 170.47, 170.56, 170.86, 170.91. Anal. Calcd for $C_{48}H_{68}N_6O_{22}$ (1081.08): C, 53.28; N, 7.77; H, 6.29. Found: C, 53.25; N, 7.78; H, 6.30. MS (HRMS) *m/z* 1080.6094 $(M)^+$, *m/z* 103.6351 $(M+Na)^+$.

4.5. ^{1}H NMR studies

All ^{1}H NMR studies were carried out on a Brüker DPX 300 MHz spectrometer at 300 K. Compounds concentrations were taken in the range of 1–10 mmol in $CDCl_3$ and $(CD_3)_2SO$.

4.6. Mass spectrometry

Mass spectra were recorded on a Hewlett Packard Series 1100MSD mass spectrometer by positive mode electrospray ionization.

4.7. Polarimeter

PerkinElmer instrument. Model 341 LC Polarimeter.

4.8. Wide angle X-ray diffraction study

The WAXS patterns were made on the gel of 1% (w/v) of dendrimers **1** and **2** in *ortho*-dichlorobenzene. The experiment was carried out in a Seifert X-ray diffractometer (C 3000) with a parallel beam optics attachment. The instrument was operated at a 35 kV voltage and 30 mA current and was calibrated with a standard silicon sample. The sample was scanned from 2° to 50° 2θ at the step scan mode (step size 0.03°, preset time 2 s) and the diffraction pattern was recorded using a scintillation scan detector.

4.9. Scanning electron microscopic study

Morphologies of all reported dendritic gels were investigated using field emission scanning electron microscopy (FE-SEM). For SEM study, the gel materials were dried and gold coated. Then the micrographs were taken in a SEM apparatus (Jeol Scanning Microscope-JSM-6700F).

4.10. Transmission electron microscopic study

The morphologies of the reported gels were investigated using transmission electron microscope (TEM). Transmission electron microscopic studies were done by placing a small amount of gel (at its minimum gelation concentration) of the corresponding compounds on carbon-coated copper grids (300 mesh) and dried by slow evaporation. The grid was then allowed to dry in vacuum at 30 °C for 2 days. Images were taken by JEM-2010 electron microscope and FEI (Tecnai spirit) instrument.

4.11. Freeze fracture transmission electron microscopic studies

Transmission electron microscopy (TEM) was performed with a Philips CM12 microscope operating at 120 kV. The gel samples were placed between two copper holders and rapidly frozen in liquid nitrogen. The sample was kept frozen and transferred into a freeze-fracture apparatus (developed by Dr. J.-C. Homo) where the sample was cleaved. Pt was evaporated onto the sample under 45° angle, and then carbon under a 90° angle respective to the surface. The sample was warmed to room temperature and the replica was rinsed with chloroform and deposited on 400 mesh grids.

4.12. Variable temperature IR (VT-IR) spectroscopy

FTIR spectra were recorded on a Bruker Vertex 70 spectrophotometer equipped with a thermostatic cell holder and a temperature-controlling unit (Specac West 6100+). The gels were placed in a NaCl cell with an optical path of 0.1 mm.

Acknowledgements

G.P. wishes to acknowledge the CSIR, New Delhi, India for financial assistance.

References and notes

1. (a) Terech, P.; Weiss, R. G. *Chem. Rev.* **1997**, *97*, 3133–3159; (b) Gronwald, O.; Snip, E.; Shinkai, S. *Curr. Opin. Colloid Interface Sci.* **2002**, *7*, 148–156; (c) Oda, R.; Huc, I.; Candau, S. J. *Angew. Chem., Int. Ed.* **1998**, *37*, 2689–2691; (d) Abdallah, D. J.; Weiss, R. G. *Adv. Mater.* **2000**, *12*, 1237–1247; (e) Shimizu, T. *Polym. J.* **2003**, *35*, 1–22; (f) Sangeetha, N. M.; Maitra, U. *Chem. Soc. Rev.* **2005**, *34*, 821–836.
2. (a) Yoha, K.; Amanokura, N.; Ono, Y.; Akao, T.; Shinmori, H.; Takeuchi, M.; Shinkai, S.; Reinhout, D. N. *Chem.—Eur. J.* **1995**, *5*, 2722–2729; (b) Yoza, K.; Ono, Y.; Yoshihara, K.; Akao, T.; Shinmori, H.; Takeuchi, M.; Shinkai, S.; Reinhoudt, D. N. *Chem. Commun.* **1998**, 907–908; (c) Schmidt, R.; Michel, M.; Schmutz, M.; Decher, G.; Mésini, P. J. *Langmuir* **2002**, *18*, 5668–5672; (d) Schmidt, R.; Adam, F. B.; Michel, M.; Schmutz, M.; Decher, G.; Mésini, P. J. *Tetrahedron Lett.* **2003**, *44*, 3171–3174; (e) de Loops, M.; van Esch, J.; Kellogg, R. M.; Feringa, B. L. *Angew. Chem., Int. Ed.* **2001**, *40*, 613–616; (f) Schoonbeek, F. S.; van Esch, J. H.; Hulst, R.; Kellogg, R. M.; Feringa, B. L. *Chem.—Eur. J.* **2000**, *6*, 2633–2643; (g) Jeong, Y.; Hanabusa, K.; Masunaga, H.; Akiba, I.; Miyoshi, K.; Sakurai, S.; Sakurai, K. *Langmuir* **2005**, *21*, 586–594; (h) Moniruzzaman, M.; Sundarajan, P. R. *Langmuir* **2005**, *21*, 3802–3807; (i) Sangeetha, N. M.; Balasubramanian, R.; Maitra, U.; Ghosh, S.; Raju, A. R. *Langmuir* **2002**, *18*, 7154–7157; (j) Willemen, H. M.; Marcelis, A. T. M.; Sudholter, E. J. R.; Bouwman, W. G.; Deme, B.; Terech, P. *Langmuir* **2004**, *20*, 2075–2080.
3. (a) Whitesides, G. M.; Grzybowski, B. A. *Science* **2002**, *295*, 2418–2421; (b) Hamley, I. W. *Angew. Chem., Int. Ed.* **2003**, *42*, 1692–1712; (c) Elemans, J. A. A. W.; Rowan, A. E.; Nolte, R. J. M. *J. Mater. Chem.* **2003**, *13*, 2661–2670; (d) An, B.-K.; Lee, D.-S.; Lee, J.-S.; Park, Y.-S.; Song, H.-S.; Park, S. Y. *J. Am. Chem. Soc.* **2004**, *126*, 10232–10233.
4. (a) Xing, B.; Choi, M.-F.; Xu, B. *Chem. Commun.* **2002**, 362–363; (b) Ihara, H.; Sakurai, T.; Yamada, T.; Hashimoto, T.; Takafuji, M.; Sagawa, T.; Hachisako, H. *Langmuir* **2002**, *18*, 7120–7123; (c) Beck, J. B.; Rowan, S. J. *J. Am. Chem. Soc.* **2003**, *125*, 13922–13923; (d) Ziessel, R.; Pickaert, G.; Camerel, F.; Donnio, B.; Guillon, D.; Cesario, M.; Prangé, T. *J. Am. Chem. Soc.* **2004**, *126*, 12403–12413; (e) Kuroiwa, K.; Shibata, T.; Takada, A.; Nemoto, N.; Kimizuka, N. *J. Am. Chem. Soc.* **2004**, *126*, 2016–2021.
5. (a) Sugiyasu, K.; Numata, M.; Fujita, N.; Park, S. M.; Yun, Y. J.; Kim, B. H.; Shinkai, S. *Chem. Commun.* **2004**, 1996–1997; (b) Sugiyasu, K.; Fujita, N.; Takeuchi, M.; Yamada, S.; Shinkai, S. *Org. Biomol. Chem.* **2003**, *1*, 895–899; (c) Kawano, S.; Fujita, N.; Shinkai, S. *Chem. Commun.* **2003**, 1352–1353; (d) Pozzo, J.-L.; Desvergne, J.-P.; Clavier, G. M.; Bouas-Laurent, H.; Jones, P. G.; Perlstein, J. *J. Chem. Soc., Perkin Trans. 2* **2001**, 824–826; (e) Placin, F.; Desvergne, J.-P.; Lassègues, J.-C. *Chem. Mater.* **2001**, *13*, 117–121; (f) Xue, P.; Lu, R.; Li, D.; Jin, M.; Bao, C.; Zhao, Y.; Wang, Z. *Chem. Mater.* **2004**, *16*, 3702–3707; (g) Jung, J. H.; Kobayashi, H.; Masuda, M.; Shimizu, T.; Shinkai, S. *J. Am. Chem. Soc.* **2001**, *123*, 8785–8789; (h) Lu, L.; Weiss, R. G. *Chem. Commun.* **1996**, 2029–2030; (i) Lin, Y.-C.; Kachar, B.; Weiss, R. G. *J. Am. Chem. Soc.* **1989**, *111*, 5542–5551; (j) George, M.; Snyder, S. L.; Terech, P.; Glinka, C. J.; Weiss, R. G. *J. Am. Chem. Soc.* **2003**, *125*, 10275–10283; (k) George, M.; Weiss, R. G. *Chem. Mater.* **2003**, *15*, 2879–2888; (l) Abdallah, D. J.; Lu, L.; Weiss, R. G. *Chem. Mater.* **1999**, *11*, 2907–2911; (m) Abdallah, D. J.; Weiss, R. G. *Langmuir* **2000**, *16*, 352–355.
6. (a) Jung, J. H.; Nakashima, K.; Shinkai, S. *Nano Lett.* **2001**, *1*, 145–148; (b) Jung, J. H.; Kobayashi, H.; van Bommel, K. J. C.; Shinkai, S.; Shimizu, T. *Chem. Mater.* **2002**, *14*, 1445–1447; (c) Xue, P.; Lu, R.; Huang, Y.; Jin, M.; Tan, C.; Bao, C.; Wang, Z.; Zhao, Y. *Langmuir* **2004**, *20*, 6470–6475; (d) Xue, P.; Lu, R.; Li, D.; Jin, M.; Tan, C.; Bao, C.; Wang, Z.; Zhao, Y. *Langmuir* **2004**, *20*, 11234–11239.
7. Shumburo, A.; Biewer, M. C. *Chem. Mater.* **2002**, *14*, 3745–3750.
8. Ray, S.; Das, A. K.; Banerjee, A. *Chem. Commun.* **2006**, 2816–2818.
9. (a) Sugiyasu, K.; Fujita, N.; Shinkai, S. *Angew. Chem., Int. Ed.* **2004**, *43*, 1229–1233; (b) Ajayaghosh, A.; George, S. J.; Praveen, V. K. *Angew. Chem., Int. Ed.* **2003**, *42*, 332–335.

10. van Esch, J. H.; Feringa, B. L. *Angew. Chem., Int. Ed.* **2000**, *39*, 2263–2266.
11. Wilder, E. A.; Wilson, K. S.; Quinn, J. B.; Skrtic, D.; Antonucci, J. M. *Chem. Mater.* **2005**, *17*, 2946–2952.
12. Kubo, W.; Kitamura, T.; Hanabusa, K.; Wada, Y.; Yanagida, S. *Chem. Commun.* **2002**, 374–377.
13. (a) Kanie, K.; Sugimoto, T. *Chem. Commun.* **2004**, 1584–1585; (b) Raj, C. R.; Jana, B. K. *Chem. Commun.* **2005**, 2005–2007; (c) Love, C. S.; Chechik, V.; Smith, D. K.; Wilson, K.; Ashworth, I.; Brennan, C. *Chem. Commun.* **2005**, 1971–1973; (d) Kim, J.; Altreute, D. H.; Clark, D. S.; Dordick, J. S. *J. Am. Oil Chem. Soc.* **1998**, *75*, 1109–1113.
14. Smith, D. K. *Adv. Mater.* **2006**, *18*, 2773–2778.
15. (a) Tomalia, D. A. *Aldrichimica Acta* **2004**, *37*, 39–57; (b) Frechet, J. M. J. *J. Polym. Sci., Part A* **2003**, *41*, 3713–3725.
16. (a) Newkome, G. R.; Baker, G. R.; Saunders, M. J.; Russo, P. S.; Gupta, V. K.; Yao, Z. Q.; Miller, J. E.; Bouillion, K. *J. Chem. Soc., Chem. Commun.* **1986**, 752–753; (b) Newkome, G. R.; Baker, G. R.; Arai, S.; Saunders, M. J.; Russo, P. S.; Theriot, K. J.; Moorefield, C. N.; Rogers, L. E.; Miller, J. E.; Lieux, T. R.; Murray, M. E.; Phillips, B.; Pascal, L. *J. Am. Chem. Soc.* **1990**, *112*, 8459–8465; (c) Newkome, G. R.; Lin, X. F.; Yaxiong, C.; Escamilla, G. H. *J. Org. Chem.* **1993**, *58*, 3123–3129; (d) Newkome, G. R.; Moorefield, C. N.; Baker, G. R.; Behera, R. K.; Escamilla, G. H.; Saunders, M. J. *Angew. Chem., Int. Ed. Engl.* **1992**, *31*, 917–919; (e) Yu, K. H.; Russo, P. S.; Younger, L.; Henk, W. G.; Hua, D. W.; Newkome, G. R.; Baker, G. *J. Polym. Sci., Polym. Phys.* **1997**, *35*, 2787–2793.
17. (a) Jang, W. D.; Jiang, D. L.; Aida, T. *J. Am. Chem. Soc.* **2000**, *122*, 3232–3233; (b) Jang, W. D.; Aida, T. *Macromolecules* **2003**, *36*, 8461–8469.
18. Zhang, W.; Gonzalez, S. O.; Simanek, E. E. *Macromolecules* **2002**, *35*, 9015–9021.
19. (a) Mulders, S. J. E.; Brouwer, A. J.; Liskamp, R. M. J. *Tetrahedron Lett.* **1997**, *38*, 3085–3088; (b) Prevote, D.; Le, R.-G. S.; Caminade, A.-M.; Masson, S.; Majoral, J.-P. *Synthesis* **1997**, 1199–1207; (c) Kayser, B.; Altman, J.; Beck, W. *Chem.—Eur. J.* **1999**, *5*, 754–758.
20. (a) Sadler, K.; Tam, J. P. *Rev. Mol. Biotechnol.* **2002**, *90*, 195–229; (b) Kolhe, P.; Misra, E.; Kannan, S.; L-Lai, M.; Kannan, R. M. *Int. J. Pharm.* **2003**, *259*, 143–160.
21. Smith, D. K.; Diederich, F. *Chem.—Eur. J.* **1998**, *4*, 1353–1361.
22. (a) Hirst, A. R.; Smith, D. K.; Feiters, M. C.; Geurts, H. P. M. *Langmuir* **2004**, *20*, 7070–7077; (b) Love, C. S.; Hirst, A. R.; Chechik, V.; Smith, D. K.; Ashworth, I.; Brennan, C. *Langmuir* **2004**, *20*, 6580–6585; (c) Partridge, K. S.; Smith, D. K.; Dykes, G. M.; McGrail, P. T. *Chem. Commun.* **2001**, 319–320; (d) Hirst, A. R.; Smith, D. K.; Feiters, M. C.; Geurts, H. P. M.; Wright, A. C. *J. Am. Chem. Soc.* **2003**, *125*, 9010–9011; (e) Hirst, A. R.; Smith, D. K.; Feiters, M. C.; Geurts, H. P. M. *Chem.—Eur. J.* **2004**, *10*, 5901–5910.
23. Ranganathan, D.; Kurur, S.; Gilardi, R.; Karle, I. L. *Biopolymers* **2000**, *54*, 289–295.
24. (a) Ji, Y.; Luo, Y.-F.; Jia, X.-R.; Chen, E.-Q.; Huang, Y.; Ye, C.; Wang, B.-B.; Zhou, Q.-F.; Wei, Y. *Angew. Chem., Int. Ed.* **2005**, *44*, 6025–6029; (b) Li, Y.; Wang, T.; Liu, M. *Tetrahedron* **2007**, *63*, 7468–7473.
25. (a) Kim, C.; Kim, K. T.; Chang, Y. H.; Song, H.; Cho, T. Y.; Jeon, H. J. *J. Am. Chem. Soc.* **2001**, *123*, 5586–5587; (b) Kim, C.; Lee, S. J.; Lee, I. H.; Kim, K. T. *Chem. Mater.* **2003**, *15*, 3638–3642.
26. Bodanszky, M.; Bodanszky, A. *The Practice of Peptide Synthesis*; Springer: New York, NY, 1984; pp 1–282.
27. Garner, M. C.; Terech, P.; Aiiegraud, J.-J.; Mistrot, B.; Nguyen, P.; de Geyer, A.; Rivera, D. *J. Chem. Soc., Faraday Trans.* **1998**, *94*, 2173–2179.
28. (a) Li, Y.; Yan, D.; Zhou, E. *Colloid Polym. Sci.* **2002**, *280*, 124–129; (b) Skrovanek, D. J.; Painter, P. C.; Coleman, M. M. *Macromolecules* **1986**, *19*, 699–705.
29. Spencer, J. N.; Berger, S. K.; Powell, C. R.; Henning, B. D.; Furman, G. S.; Loffredo, W. M.; Rydberg, E. M.; Neubert, R. A.; Shoop, C. E.; Blauch, D. N. *J. Phys. Chem.* **1981**, *85*, 1236–1241.
30. Huang, X.; Raghavan, R. S.; Terech, P.; Weiss, G. R. *J. Am. Chem. Soc.* **2006**, *128*, 15334–15352.
31. (a) Ramachandran, G. N.; Kartha, G. *Nature* **1955**, *179*, 593–594; (b) Eyre, D. R. *Science* **1980**, *207*, 1315–1322; (c) Pouling, L.; Corey, R. B.; Branson, H. R. *Proc. Natl. Acad. Sci. U.S.A.* **1951**, *37*, 205–211; (d) Watson, J. D.; Crick, F. H. C. *Nature* **1953**, *171*, 737–738.
32. (a) Hirst, A. R.; Smith, D. K.; Harrington, J. P. *Chem.—Eur. J.* **2005**, *11*, 6552–6559; (b) Zhou, Y.; Yi, T.; Li, T.; Zhou, Z.; Li, F.; Huang, W.; Huang, C. *Chem. Mater.* **2006**, *18*, 2974–2981; (c) Zhu, G.; Dordick, J. S. *Chem. Mater.* **2006**, *18*, 5988–5995.
33. Malik, S.; Kawano, S.; Fujita, N.; Shinkai, S. *Tetrahedron* **2007**, *63*, 7326–7333.